



In Silico Analysis of miRNA-mediated ceRNAs as Potential Molecular Biomarkers in Glioblastoma

Orcun Avsar ¹

1 Department of Molecular Biology and Genetics, Faculty of Science and Art, Hitit University, Corum, Turkey

Received: 14.04.2021; Revised: 04.08.2021; Accepted: 12.08.2021

Abstract

Objectives: Glioblastoma multiforme (GBM) is defined as the most frequent and lethal form of the primary brain tumors in the central nervous system (CNS) in adults. Recent studies have focused on the identification of the new targets for the diagnosis and treatment of GBM and resulted in great interest for miRNAs due to their regulatory effects in cancer pathogenesis. Thus, we aimed to characterize novel molecular biomarkers for GBM by computational analysis.

Methods: 118 miRNAs that are clinically related with glioblastoma and proven by experimentally were exported through miRTarBase database. 1016 genes projected by these 118 miRNAs were determined via ComiR database. Subsequently, the genes with transcribed ultraconserved regions (T-UCRs) in their exonic regions were designated and the genes which have potential competing endogenous RNA (ceRNA) activities were extracted. Genes with remarkable expression profile differences between glioblastoma and normal brain tissues among ceRNAs that are associated with glioblastoma involving T-UCR were identified.

Results: The statistical analysis of the correlation between PBX3 and NRXN3 genes and glioblastoma was carried out by Spearman correlation test. PBX3 and NRXN3 expression was significantly higher and lower in glioblastoma than in normal brain tissues, respectively. On the other hand, the other genes did not have any remarkable differential expression pattern.

Conclusion: Based on the findings of the current study, it is determined that NRXN3 acts as a tumor suppressor gene and NRXN3 gene is downregulated in GBM. PBX3 gene functions as an oncogene and is upregulated in GBM.

Keywords: Glioblastoma, GBM, miRNA, ceRNA, T-UCR.

DOI: 10.5798/dicletip.987908

Correspondence / Yazışma Adresi: Orcun Avsar, Department of Molecular Biology and Genetics, Faculty of Science and Art, Hitit University, Corum, Turkey e-mail: orcunavsar.gen@gmail.com

Glioblastomada Potansiyel Moleküler Biyobelirteçler Olarak miRNA Aracılı ceRNA'ların *İn Siliko* Analizi

Öz

Amaç: Glioblastoma multiforme (GBM), yetişkinlerde santral sinir sistemi (SSS)'ndeki primer beyin tümörlerinin en sık görülen ve en öldürücü tipi olarak tanımlanmaktadır. Son yıllardaki çalışmalar, GBM'nin teşhisi ve tedavisi için yeni hedeflerin tanımlanmasına odaklanmış ve kanser patogenezindeki düzenleyici etkileri nedeniyle miRNA'lara büyük ilgi uyandırmıştır. Bu nedenle, bu çalışmada GBM için yeni moleküler biyobelirteçlerin hesaplamalı analizlerle tanımlanması amaçlanmıştır.

Yöntemler: Glioblastoma ile klinik olarak ilişkili olan ve deneysel olarak kanıtlanmış 118 miRNA, miRTarBase veri tabanından elde edildi. Elde edilen 118 miRNA tarafından hedeflenen 1016 gen ComiR veri tabanı aracılığıyla belirlendi. Akabinde, ekzonik bölgelerinde transkribe edilmiş ultra-korunmuş bölgelere (T-UCR) sahip genler belirlendi ve potansiyel olarak endojen rekabetçi RNA (ceRNA) aktivitelerine sahip olan genler ekstrakte edildi. T-UCR içeren glioblastoma ile ilişkili ceRNA'lar arasından glioblastoma ve normal beyin dokuları arasında önemli ekspresyon profili farklılıklarına sahip genler tanımlandı.

Bulgular: PBX3 ve NRXN3 genleri ile glioblastoma arasındaki korelasyonun istatistiksel analizi Spearman korelasyon testi ile gerçekleştirildi. Normal beyin dokularına göre glioblastomada PBX3 gen ekspresyonu daha yüksek iken NRXN3 gen ekspresyonu daha düşüktü. Diğer taraftan, diğer genler anlamlı farklılık gösteren ekspresyon paternine sahip değildi.

Sonuç: Mevcut çalışmanın bulgularına göre, NRXN3 geninin tümör baskılayıcı olarak işlev gördüğü ve GBM'de downregüle edildiği ve PBX3 geninin onkogen olarak görev aldığı ve GBM'de upregüle edildiği belirlendi.

Anahtar kelimeler: Glioblastoma, GBM, miRNA, ceRNA, T-UCR.

INTRODUCTION

Glioblastoma is classified as primary glioblastoma multiforme (GBM) which is seen in 80% of cases with the onset approximately at age 62, and secondary GBM which is derived from oligodendrogliomas or astrocytomas with the onset at age 45 on average¹. GBM is defined as the most frequent and lethal form of the primary brain tumors in the central nervous system (CNS) in adults and classified as Grade IV by the World Health Organization². Approximately 1/3 of primary brain tumors is glioblastoma multiforme. The diagnosis and treatment of GBM is challenging and treatment options have not altered over many years even its high frequency³.

MicroRNAs (miRNAs) that are non-coding and short (18-22 nucleotides) RNA molecules are expressed in the cells of many organisms. miRNAs modulate gene and protein expression by degrading target mRNA or blocking translation. Thousands of miRNA genes have

been designated in the genomes of many organisms such as plants, animals. Approximately 60% of the human genome and nearly every gene clusters are estimated to be regulated by miRNAs. MicroRNAs are key players of numerous biological functions and disruption of the function of miRNAs cause to many diseases such as cancer and neuropsychiatric diseases. Moreover, in recent years, miRNA regulation of physiology of cells, miRNA therapeutics, xenomiRs, and miRNA biomarkers have been receiving a great deal of attention by researchers^{4,5}.

Competing endogenous RNAs (ceRNAs) are transcripts that compete for microRNA binding, modulating each other's functions post-transcriptionally. miRNAs bind to microRNA response elements (MREs) in the 3'UTRs of target mRNA. ceRNAs consist of various RNA transcript types such as protein-encoding mRNAs, circRNAs, pseudogenes, and lncRNAs. It has been proposed that many RNAs may interact with each other via MREs. The

repressive action of miRNA is deactivated by “ceRNAs” or “miRNA sponges”. The ceRNAs which have many MREs for a miRNA show multiple interactions and it is resulted with a complex regulatory network. Dysregulation of ceRNA network leads to various human diseases such as cancer. ceRNAs are key players of carcinogenesis and molecular pathways are affected by ceRNA interactions. Hence, underlying molecular mechanisms of cancer may be elucidated by the analysis of ceRNAs^{6,7}.

Ultra-conserved regions (UCRs) are non-coding DNA sequences and conserved among mice, rats, and human beings. UCRs were discovered in mice, rats, and human genomes by bioinformatics tools in 2004. More than 90% of ultra-conserved regions are transcribed (T-UCRs) in normal tissues and are modulated at the level of transcription in carcinogenesis. The expression levels of T-UCRs have tissue-specific pattern. Recent studies conducted with genome-wide expression profiling approach have demonstrated that T-UCRs show divergent profiles in various cancer types and support their roles in tumorigenesis⁸.

One of the most aggressive cancers, glioblastoma is challenging for treatment. Recent studies have focused on the determination of the new targets for the diagnosis and treatment of GBM and resulted in great interest for miRNAs due to their regulatory effects in normal conditions and cancer pathogenesis. According to the properties of miRNAs, it is aimed to identify novel molecular biomarkers for GBM by in silico analysis in this study.

METHODS

miRNA selection

First of all, the miRNAs that are implicated in the pathogenesis of glioblastoma were selected. In this regard, one hundred and eighteen miRNAs that are clinically related with glioblastoma and proven by experimentally were exported

through miRTarBase database. Extensive information about experimentally verified miRNA-target interactions was obtained from the miRTarBase database. Scientists can apply for the database in order to confirm novel targets of miRNA^{9,10}.

miRNA-mediated ceRNAs analysis

One thousand sixteen genes projected by these one hundred and eighteen miRNAs were determined using the ComiR database. The genes with ComiR score greater than 0.8685 were taken into account in this study. ComiR is an online web server for combinatorial miRNA target estimation and has a free access for academic users. ComiR estimates the potential of being targeted by a group of microRNAs for a mRNA in fly, mouse, worm or human genomes and each one may have zero, one or more targets on its 3'UTR. In identification the modulator potential of a mRNA from a cluster of miRNAs, ComiR uses the levels of miRNA expression which are provided by the users in a combination of relevant machine learning techniques and thermodynamic modeling in order to make more certain estimations. For each gene, the tool indicates the possibility of being functional target of a group of miRNAs according to the relative miRNA expression levels¹⁰⁻¹². It is expected that RNA transcripts of the given genes have potential ceRNA activities for the microRNAs and this regulation may occur via miRNA-sponging mechanism¹³.

Matching of ceRNAs with the genes containing T-UCR

Ultra-conserved regions (UCRs) in the human genome were determined by Bejerano et al.¹⁴. The genes involving these regions classified as downstream, upstream, and exonic based on the localization within the gene¹⁴. In this study, the genes with T-UCR in their exonic regions were designated and the genes which have potential ceRNA activities were extracted in the previous analysis.

Analysis of differential gene expression between glioblastoma and normal brain tissues

The genes with remarkable expression differences between brain tissue and glioblastoma multiforme from glioblastoma-associated ceRNAs involving T-UCR were designated via Gene Expression Profiling Interactive Analysis (GEPIA) database^{10,12}. GEPIA that is user-friendly web tool delivers normal and cancer gene expression and interactive analysis data¹⁵.

Analysis of the correlation between PBX3 and NRXN3 genes in glioblastoma

Analysis of differential gene expression ensures to find the tumor-specific genes by comparing normal and tumor groups^{10,12}. The statistical analysis of the relationship between PBX3 and

NRXN3 genes and glioblastoma was carried out by the use of Spearman correlation test.

RESULTS

In the current study, one hundred and eighteen miRNAs that are clinically associated with glioblastoma and proven by experimentally by the use of miRTarBase database are shown in Table I. One thousand sixteen genes that are simultaneously targeted by these 118 miRNAs were shown in supplementary I. The genes with ComiR score greater than 0.8685 were taken into account in this study. The genes which include T-UCR in exons based on the study of Bejerano et al.¹⁴ was determined and afterwards, the ones which have potential ceRNA activities were extracted and are shown in Table II.

Supplementary I: The genes targeted by these 118 glioblastoma-associated miRNAs simultaneously.

Gene ID	ComiR equal abundance score				
<i>SCYL3</i>	0.9157	<i>HFE</i>	0.8686	<i>ADAMTS6</i>	0.9156
<i>LASP1</i>	0.914	<i>SLC7A14</i>	0.8689	<i>H6PD</i>	0.8693
<i>CFLAR</i>	0.9162	<i>NUDCD3</i>	0.8692	<i>NEDD4L</i>	0.8688
<i>SARM1</i>	0.8693	<i>IGF1</i>	0.8691	<i>KIAA2022</i>	0.8689
<i>FKBP4</i>	0.9142	<i>PRDM11</i>	0.9222	<i>HEBP2</i>	0.8695
<i>THSD7A</i>	0.8691	<i>NRXN3</i>	0.8686	<i>MPHOSPH9</i>	0.9133
<i>KMT2E</i>	0.8685	<i>SLC45A4</i>	0.9155	<i>SIKE1</i>	0.8689
<i>ZNF263</i>	0.9143	<i>GRAMD1B</i>	0.8689	<i>FOXN3</i>	0.869
<i>MAP3K9</i>	0.916	<i>NDUFS1</i>	0.8695	<i>AP5M1</i>	0.9226
<i>TTC22</i>	0.9112	<i>KPNA6</i>	0.8688	<i>EIF2AK2</i>	0.8695
<i>GAS7</i>	0.9159	<i>AGPAT4</i>	0.8692	<i>KMT2C</i>	0.8697
<i>E2F2</i>	0.9151	<i>POU2F2</i>	0.9223	<i>ATP2B4</i>	0.9146
<i>CDKL5</i>	0.8693	<i>SNX1</i>	0.8694	<i>RIOK2</i>	0.9133
<i>ST3GAL1</i>	0.8685	<i>IKZF2</i>	0.9157	<i>BCAT1</i>	0.8693
<i>REV3L</i>	0.9225	<i>UBA6</i>	0.869	<i>MON2</i>	0.9224
<i>IDS</i>	0.8685	<i>GAB2</i>	0.9137	<i>EPN1</i>	0.9162
<i>ZNF200</i>	0.9121	<i>DAPK2</i>	0.869	<i>ZNF275</i>	0.9153
<i>LRRC23</i>	0.9112	<i>ADAM28</i>	0.9155	<i>HIPK2</i>	0.8695
		<i>HDAC9</i>	0.9155	<i>UHRF1BP1</i>	0.8686
		<i>SNX29</i>	0.8691	<i>GNAI3</i>	0.9162
		<i>RSF1</i>	0.8691	<i>WDR3</i>	0.9224

<i>PKN2</i>	0.9145
<i>SLK</i>	0.9144
<i>MTHFD2</i>	0.9148
<i>SLC9A7</i>	0.8691
<i>CD84</i>	0.8694
<i>ATXN3</i>	0.9237
<i>DNTTIP2</i>	0.9149
<i>RRP15</i>	0.869
<i>ROCK1</i>	0.8689
<i>PSME4</i>	0.9155
<i>NEDD4</i>	0.8691
<i>GNB5</i>	0.9159
<i>PTPN3</i>	0.9152
<i>EXOC5</i>	0.9159
<i>RAD18</i>	0.8685
<i>MGAT4A</i>	0.8688
<i>ZFYVE26</i>	0.9223
<i>RPS6KA6</i>	0.8693
<i>SMC1A</i>	0.9234
<i>CHFR</i>	0.8694
<i>TRHDE</i>	0.9161
<i>P4HA2</i>	0.9114
<i>IGF2BP2</i>	0.9128
<i>MGLL</i>	0.9145
<i>IPCEF1</i>	0.869
<i>ADD2</i>	0.8693
<i>RASAL2</i>	0.9162
<i>ZNF37A</i>	0.8688
<i>FNDC3B</i>	0.9155
<i>WDR62</i>	0.8688
<i>BCAP29</i>	0.9151
<i>SEC31B</i>	0.9151
<i>RBM7</i>	0.8689
<i>RBMS2</i>	0.8694
<i>PLXNA2</i>	0.869
<i>PAG1</i>	0.8686
<i>MBNL3</i>	0.9162
<i>PPP1R12B</i>	0.8696

<i>DNAJC10</i>	0.9162
<i>DCX</i>	0.9159
<i>ACER3</i>	0.8687
<i>PIK3C3</i>	0.8685
<i>N4BP2</i>	0.8691
<i>RUNX1T1</i>	0.8687
<i>RIF1</i>	0.8694
<i>RAB21</i>	0.8696
<i>CDH7</i>	0.9161
<i>MEF2C</i>	0.9134
<i>BZW1</i>	0.9119
<i>PGR</i>	0.8695
<i>FAM135A</i>	0.9158
<i>ERC1</i>	0.8687
<i>XPO1</i>	0.869
<i>LYRM2</i>	0.9157
<i>ZNF264</i>	0.9162
<i>SSH1</i>	0.8696
<i>MAP3K4</i>	0.9134
<i>PTPN4</i>	0.8687
<i>C20orf194</i>	0.9145
<i>MAVS</i>	0.8696
<i>NOS1</i>	0.8689
<i>ZBTB25</i>	0.9161
<i>ARHGAP4</i>	0.9143
<i>GPATCH2L</i>	0.9162
<i>PCBP4</i>	0.9199
<i>ZNF268</i>	0.9224
<i>PDPR</i>	0.8686
<i>TNRC6A</i>	0.8695
<i>DTX2</i>	0.9096
<i>RGS17</i>	0.8685
<i>SNAP23</i>	0.9116
<i>AGO1</i>	0.9162
<i>GPATCH2</i>	0.9156
<i>ECHDC1</i>	0.9118
<i>CBX5</i>	0.9226
<i>FKBP5</i>	0.8692

<i>CDC5L</i>	0.9142
<i>CDC34</i>	0.9106
<i>MTAP</i>	0.9157
<i>CECR2</i>	0.915
<i>DDTL</i>	0.9106
<i>MAPK1</i>	0.8695
<i>ADRBK2</i>	0.8692
<i>TFIP11</i>	0.91
<i>RBFOX2</i>	0.8688
<i>MTMR3</i>	0.8687
<i>MIEF1</i>	0.9142
<i>KIAA0930</i>	0.9151
<i>DDHD1</i>	0.9162
<i>VTI1B</i>	0.8685
<i>SPTLC2</i>	0.8688
<i>GALNT16</i>	0.9152
<i>DICER1</i>	0.9155
<i>ZC3H14</i>	0.9162
<i>RPS6KA5</i>	0.9237
<i>KIAA0391</i>	0.9219
<i>SLC52A3</i>	0.9124
<i>ST8SIA5</i>	0.8695
<i>CEP192</i>	0.8693
<i>RNMT</i>	0.9154
<i>LIPG</i>	0.8695
<i>ANKRD12</i>	0.915
<i>MIB1</i>	0.915
<i>PGRMC1</i>	0.9103
<i>ALG13</i>	0.9151
<i>PORCN</i>	0.9126
<i>KLF8</i>	0.9149
<i>FGF14</i>	0.9161
<i>FNDC3A</i>	0.915
<i>STK24</i>	0.9235
<i>KATNAL1</i>	0.9152
<i>INTS6</i>	0.8696
<i>NFAT5</i>	0.8696
<i>LONP2</i>	0.8687

<i>CCDC113</i>	0.9147
<i>SLC7A6</i>	0.9157
<i>ESRP2</i>	0.9134
<i>MLYCD</i>	0.8694
<i>GSPT1</i>	0.8689
<i>GGA2</i>	0.9152
<i>XYLT1</i>	0.8694
<i>HOMER2</i>	0.916
<i>EHD4</i>	0.8687
<i>ATP8B4</i>	0.8687
<i>DTWD1</i>	0.8696
<i>SLC30A4</i>	0.8686
<i>MYEF2</i>	0.8689
<i>FZD3</i>	0.9226
<i>UBE2W</i>	0.9161
<i>TUBB4A</i>	0.9126
<i>AKAP8</i>	0.9139
<i>AVL9</i>	0.8687
<i>CDK6</i>	0.8694
<i>ITGB8</i>	0.869
<i>TTC26</i>	0.914
<i>TFEC</i>	0.8685
<i>HOXA1</i>	0.9116
<i>PLEKHA8</i>	0.9158
<i>AP1S1</i>	0.9112
<i>C1GALT1</i>	0.8688
<i>TMEM106B</i>	0.8696
<i>FKTN</i>	0.9224
<i>TGFBR1</i>	0.915
<i>AKNA</i>	0.9146
<i>KCNT1</i>	0.9222
<i>RGP1</i>	0.8686
<i>ABCA2</i>	0.8685
<i>CCNJ</i>	0.9133
<i>PLEKHA1</i>	0.8696
<i>BMPR1A</i>	0.916
<i>CPEB3</i>	0.9158
<i>FBXL20</i>	0.8695

<i>INTS2</i>	0.9114
<i>LUC7L3</i>	0.8688
<i>GABRA4</i>	0.8695
<i>CLNK</i>	0.9142
<i>CTSC</i>	0.869
<i>DTX4</i>	0.9148
<i>CCND1</i>	0.9122
<i>CBL</i>	0.9161
<i>CARS</i>	0.913
<i>SOX6</i>	0.8691
<i>CAPRIN2</i>	0.9159
<i>DUSP16</i>	0.9143
<i>C12orf49</i>	0.8694
<i>TBC1D30</i>	0.9156
<i>CNOT2</i>	0.9129
<i>KRR1</i>	0.869
<i>ST8SIA1</i>	0.869
<i>FRK</i>	0.8696
<i>SOD2</i>	0.8692
<i>RNF8</i>	0.8687
<i>ZNF451</i>	0.8694
<i>ASCC3</i>	0.9139
<i>KIAA1244</i>	0.8694
<i>SLC16A10</i>	0.9225
<i>IMPG1</i>	0.869
<i>GHR</i>	0.9153
<i>COL4A3BP</i>	0.9149
<i>PRLR</i>	0.9225
<i>SKP1</i>	0.9161
<i>CPEB4</i>	0.9146
<i>KPNA1</i>	0.9156
<i>UBE3A</i>	0.9221
<i>XRN1</i>	0.9154
<i>BBX</i>	0.9159
<i>KIAA1257</i>	0.8685
<i>HEMK1</i>	0.9241
<i>ACVR2B</i>	0.9161
<i>ABCC5</i>	0.9144

<i>KLHL24</i>	0.9152
<i>INO80D</i>	0.8696
<i>TTL</i>	0.9161
<i>TFCP2L1</i>	0.8693
<i>DNAJC27</i>	0.8685
<i>APC2</i>	0.9142
<i>TTC31</i>	0.9139
<i>PAPOLG</i>	0.8685
<i>ELMOD3</i>	0.9131
<i>GGCX</i>	0.8692
<i>ZNF142</i>	0.8691
<i>HDLBP</i>	0.9124
<i>PLCL1</i>	0.8692
<i>KYNU</i>	0.8696
<i>AAK1</i>	0.9162
<i>ARID3A</i>	0.9209
<i>PLEKHA3</i>	0.9237
<i>TNR</i>	0.8694
<i>GPX7</i>	0.9113
<i>KCNC4</i>	0.8697
<i>MEF2D</i>	0.9156
<i>C1orf21</i>	0.9162
<i>TROVE2</i>	0.9155
<i>MTR</i>	0.8691
<i>RIMS3</i>	0.869
<i>AKT3</i>	0.8688
<i>CTBS</i>	0.8688
<i>TMED5</i>	0.8686
<i>DR1</i>	0.8695
<i>PTBP2</i>	0.8696
<i>DIEXF</i>	0.8693
<i>SLC5A9</i>	0.9113
<i>SGIP1</i>	0.8688
<i>ADGB</i>	0.916
<i>MED28</i>	0.9162
<i>SLC16A7</i>	0.8696
<i>DCLRE1B</i>	0.9138
<i>CCND2</i>	0.9222

<i>CYP20A1</i>	0.8695
<i>TRPM6</i>	0.9135
<i>TRIM67</i>	0.9157
<i>FBXW2</i>	0.9161
<i>RBM18</i>	0.8686
<i>ONECUT2</i>	0.9241
<i>YLPM1</i>	0.9152
<i>NEK9</i>	0.9154
<i>DNAL1</i>	0.8693
<i>NRDE2</i>	0.8695
<i>ZNF410</i>	0.9126
<i>YIPF4</i>	0.8695
<i>FAM178A</i>	0.9146
<i>HELLS</i>	0.9155
<i>MOB3B</i>	0.869
<i>B4GALT4</i>	0.8686
<i>ACVR2A</i>	0.9152
<i>ODF2L</i>	0.8685
<i>ZNF644</i>	0.9106
<i>SEPT7</i>	0.8689
<i>CHST3</i>	0.915
<i>SLC25A16</i>	0.8686
<i>SPRYD7</i>	0.9117
<i>NLN</i>	0.9219
<i>ATPAF1</i>	0.9145
<i>ACVR1C</i>	0.8687
<i>LPGAT1</i>	0.9224
<i>PARD6B</i>	0.9151
<i>RAB22A</i>	0.8691
<i>BCAS4</i>	0.8689
<i>STAMBP</i>	0.8687
<i>HIF3A</i>	0.9155
<i>NQO2</i>	0.916
<i>ATXN1</i>	0.8694
<i>SH3TC1</i>	0.9219
<i>ATP5S</i>	0.9225
<i>GGA3</i>	0.9154
<i>GTF3C4</i>	0.8688

<i>POLR1B</i>	0.9153
<i>THOC2</i>	0.9141
<i>MED1</i>	0.8686
<i>GPCPD1</i>	0.915
<i>TMX4</i>	0.9152
<i>AP5S1</i>	0.9155
<i>MKKS</i>	0.9155
<i>RALY</i>	0.9223
<i>CEP250</i>	0.916
<i>AMOT</i>	0.9155
<i>AGO3</i>	0.9226
<i>THRA</i>	0.9143
<i>PCNXL4</i>	0.9162
<i>MASP1</i>	0.915
<i>HELB</i>	0.9161
<i>RAP1B</i>	0.8696
<i>RAB3IP</i>	0.8691
<i>PTPRB</i>	0.869
<i>DYRK2</i>	0.9158
<i>ZNF835</i>	0.9126
<i>HIP1</i>	0.8688
<i>FOXP2</i>	0.9224
<i>MKLN1</i>	0.9161
<i>TMOD2</i>	0.8693
<i>ICE2</i>	0.9158
<i>ARPP19</i>	0.869
<i>CALML4</i>	0.9137
<i>KCNC1</i>	0.8689
<i>PRRG3</i>	0.8685
<i>ATP8B3</i>	0.9158
<i>DDA1</i>	0.9155
<i>TULP4</i>	0.8689
<i>PXDN</i>	0.9132
<i>PGPEP1</i>	0.9156
<i>ZNF557</i>	0.8687
<i>ZNF341</i>	0.9215
<i>NFATC1</i>	0.9121
<i>RAB11FIP4</i>	0.9154

<i>LRRRC41</i>	0.9107
<i>ENOSF1</i>	0.9147
<i>GRSF1</i>	0.8688
<i>PCBD2</i>	0.869
<i>SCO1</i>	0.8693
<i>STARD13</i>	0.9137
<i>LARGE</i>	0.8687
<i>MYO18B</i>	0.8687
<i>FAM83F</i>	0.8697
<i>MBD2</i>	0.9218
<i>WNT2B</i>	0.916
<i>MYCN</i>	0.9119
<i>CRB1</i>	0.9223
<i>KLRD1</i>	0.9237
<i>AGO4</i>	0.9153
<i>BTF3L4</i>	0.8685
<i>DAGLA</i>	0.9156
<i>FADS2</i>	0.9131
<i>CLOCK</i>	0.9159
<i>DZIP1</i>	0.8685
<i>MTO1</i>	0.9161
<i>ZC3H10</i>	0.8693
<i>CD164</i>	0.914
<i>REPS1</i>	0.8687
<i>USP15</i>	0.8696
<i>CPM</i>	0.8689
<i>KIAA0513</i>	0.8693
<i>SLC9A5</i>	0.9149
<i>RC3H1</i>	0.8692
<i>TTLL4</i>	0.9121
<i>ALDH1L2</i>	0.9158
<i>USP44</i>	0.9192
<i>SLC41A2</i>	0.9146
<i>ALPK3</i>	0.8687
<i>LIMD2</i>	0.9224
<i>KAT7</i>	0.8695
<i>SKIL</i>	0.922
<i>UGGT1</i>	0.9157

<i>ARHGEF39</i>	0.9131
<i>YIPF3</i>	0.9113
<i>SLC22A23</i>	0.8688
<i>TAF8</i>	0.9159
<i>CPEB2</i>	0.9205
<i>RAB30</i>	0.8694
<i>SLCO5A1</i>	0.9155
<i>TMPRSS4</i>	0.8686
<i>UNC13C</i>	0.9159
<i>CTDSPL2</i>	0.9151
<i>THBS1</i>	0.8687
<i>ITGA11</i>	0.9223
<i>ADAM10</i>	0.8695
<i>TTLL7</i>	0.869
<i>IFI44L</i>	0.9152
<i>ADAMTS14</i>	0.9123
<i>SSFA2</i>	0.9157
<i>ABI2</i>	0.8697
<i>PARP9</i>	0.9151
<i>CNOT6L</i>	0.8689
<i>KIAA1644</i>	0.922
<i>NDUFA9</i>	0.8686
<i>TARBP2</i>	0.9126
<i>ACVRL1</i>	0.913
<i>ANKRD52</i>	0.9234
<i>ZNF740</i>	0.9158
<i>WDFY2</i>	0.8691
<i>NOVA1</i>	0.9159
<i>SYT16</i>	0.8696
<i>SLC38A6</i>	0.9145
<i>NAA30</i>	0.9234
<i>RAB15</i>	0.9215
<i>TSPAN3</i>	0.9159
<i>IGF1R</i>	0.9224
<i>ABHD2</i>	0.8693
<i>NTRK3</i>	0.9226
<i>DET1</i>	0.9138
<i>ZNF710</i>	0.9147

<i>FTO</i>	0.9161
<i>NKD1</i>	0.8691
<i>GFOD2</i>	0.9156
<i>PCTP</i>	0.9129
<i>GNAL</i>	0.8685
<i>C18orf21</i>	0.9084
<i>GALNT1</i>	0.9129
<i>GAREM</i>	0.8685
<i>TP53</i>	0.913
<i>TBCD</i>	0.9108
<i>TRIM65</i>	0.9114
<i>RNF165</i>	0.9161
<i>WTIP</i>	0.8695
<i>POU2F1</i>	0.9237
<i>ABL2</i>	0.916
<i>RGS16</i>	0.9116
<i>LHX9</i>	0.9155
<i>SNX27</i>	0.8693
<i>GABPB2</i>	0.916
<i>SYT14</i>	0.8691
<i>ACP1</i>	0.9116
<i>PLEKHA6</i>	0.9156
<i>PTPN7</i>	0.9114
<i>SYT2</i>	0.8691
<i>TEX261</i>	0.9145
<i>ZC3H8</i>	0.9158
<i>KIAA1715</i>	0.8692
<i>GULP1</i>	0.869
<i>SPAG16</i>	0.922
<i>LIMD1</i>	0.9161
<i>ZNF660</i>	0.9158
<i>MUC4</i>	0.9146
<i>TBCK</i>	0.869
<i>SPATA5</i>	0.8689
<i>METTL14</i>	0.9157
<i>USP53</i>	0.9148
<i>UGT3A1</i>	0.9154
<i>SSBP2</i>	0.869

<i>PPIP5K2</i>	0.8696
<i>BDP1</i>	0.9145
<i>TNFAIP8</i>	0.9159
<i>ATG12</i>	0.9151
<i>ARHGAP26</i>	0.8693
<i>PCYOX1L</i>	0.9138
<i>G3BP1</i>	0.869
<i>GFOD1</i>	0.8691
<i>IRAK1BP1</i>	0.8687
<i>MMS22L</i>	0.9155
<i>FAXC</i>	0.8694
<i>CLVS2</i>	0.8695
<i>RNF217</i>	0.9225
<i>SHPRH</i>	0.8695
<i>PURB</i>	0.8691
<i>CASK</i>	0.8691
<i>KDM6A</i>	0.9143
<i>DIAPH2</i>	0.916
<i>FAM135B</i>	0.9154
<i>VLDLR</i>	0.916
<i>UGCG</i>	0.9136
<i>SNX30</i>	0.9221
<i>NR6A1</i>	0.9237
<i>A1CF</i>	0.9225
<i>EIF4EBP2</i>	0.8688
<i>CNNM2</i>	0.8696
<i>INTS4</i>	0.9135
<i>SOGA1</i>	0.8695
<i>PCDH15</i>	0.8689
<i>CDH8</i>	0.9154
<i>LPHN3</i>	0.916
<i>PDCD4</i>	0.913
<i>CD226</i>	0.8696
<i>FREM2</i>	0.8691
<i>DCP1B</i>	0.9121
<i>THRB</i>	0.8689
<i>GXYLT1</i>	0.9158
<i>AKAP6</i>	0.9161

<i>THRSP</i>	0.9104
<i>ADAMTS12</i>	0.9151
<i>C4orf33</i>	0.8689
<i>WWC2</i>	0.8686
<i>GABRA2</i>	0.8688
<i>GFRA1</i>	0.8695
<i>CACUL1</i>	0.8694
<i>RABGAP1L</i>	0.8687
<i>PTPN14</i>	0.8694
<i>EPG5</i>	0.8689
<i>ATP5A1</i>	0.8686
<i>GUCY1A2</i>	0.9226
<i>ZNF773</i>	0.8692
<i>FARP1</i>	0.9157
<i>ZNF117</i>	0.8685
<i>SREK1IP1</i>	0.9223
<i>SMARCA5</i>	0.8685
<i>RANBP2</i>	0.9117
<i>ASAP1</i>	0.9222
<i>PTPRD</i>	0.9149
<i>CNKSR3</i>	0.9237
<i>SREK1</i>	0.8686
<i>HS2ST1</i>	0.869
<i>MSI2</i>	0.8689
<i>CHST9</i>	0.9162
<i>OTULIN</i>	0.8685
<i>LRRK1</i>	0.9162
<i>ENAH</i>	0.9161
<i>GPR26</i>	0.8691
<i>ADAMTS5</i>	0.8688
<i>PIEZO2</i>	0.8687
<i>APOOL</i>	0.869
<i>ATP6V1C1</i>	0.9151
<i>PDZD9</i>	0.9115
<i>PPARGC1B</i>	0.9224
<i>LSM11</i>	0.8689
<i>AFF2</i>	0.8693
<i>PSD3</i>	0.8694

<i>MMP16</i>	0.8693
<i>BACH1</i>	0.9127
<i>ANKRD9</i>	0.8686
<i>UQCRB</i>	0.8688
<i>AIFM1</i>	0.9129
<i>FBXO32</i>	0.8689
<i>B3GNT7</i>	0.9134
<i>ATP2B2</i>	0.8685
<i>STEAP2</i>	0.8689
<i>HYDIN</i>	0.9151
<i>MYO1E</i>	0.8687
<i>KCNJ6</i>	0.8696
<i>TSPAN18</i>	0.9152
<i>DGKI</i>	0.8696
<i>UBN2</i>	0.8695
<i>BRAF</i>	0.8693
<i>AP3S2</i>	0.8688
<i>WIP12</i>	0.9142
<i>PAFAH2</i>	0.914
<i>XKR8</i>	0.9115
<i>EYA3</i>	0.8687
<i>CLSTN2</i>	0.8696
<i>PPP1R15B</i>	0.9142
<i>AGPAT6</i>	0.9151
<i>ELK4</i>	0.9161
<i>TNNI1</i>	0.869
<i>IGF2BP1</i>	0.9235
<i>SCUBE1</i>	0.8692
<i>STARD9</i>	0.9204
<i>ACE</i>	0.9124
<i>BSDC1</i>	0.9125
<i>ZBTB8A</i>	0.869
<i>ZNF362</i>	0.9125
<i>TRAPP10</i>	0.8685
<i>ICOSLG</i>	0.9152
<i>TAOK1</i>	0.8691
<i>MFSD12</i>	0.9099
<i>PLXDC1</i>	0.8686

<i>IKZF3</i>	0.9161
<i>ACOX1</i>	0.8688
<i>TMEM143</i>	0.9099
<i>FMNL3</i>	0.9162
<i>TREML1</i>	0.9102
<i>CCNF</i>	0.9226
<i>PRKAA2</i>	0.8693
<i>CTRC</i>	0.9147
<i>RBBP4</i>	0.916
<i>UBXN10</i>	0.8686
<i>NFIA</i>	0.8693
<i>ZNF326</i>	0.8693
<i>SLC30A7</i>	0.8689
<i>VANGL2</i>	0.914
<i>ACP6</i>	0.9234
<i>WDR26</i>	0.8686
<i>REL</i>	0.9162
<i>DISC1</i>	0.8688
<i>FAM84A</i>	0.869
<i>DUSP19</i>	0.8685
<i>SMARCAD1</i>	0.9141
<i>EOGT</i>	0.9132
<i>EIF4E3</i>	0.8694
<i>LRRRC58</i>	0.8692
<i>CCDC141</i>	0.8686
<i>ICA1L</i>	0.8692
<i>RYBP</i>	0.9155
<i>RPP14</i>	0.8692
<i>RBM47</i>	0.9146
<i>APBB2</i>	0.9158
<i>TTC14</i>	0.9158
<i>SEN2</i>	0.9151
<i>IFT122</i>	0.9153
<i>SFMBT1</i>	0.9111
<i>CDC25A</i>	0.9184
<i>INTU</i>	0.8696
<i>RNF123</i>	0.9139
<i>MFSD8</i>	0.9144

<i>WDR41</i>	0.9142
<i>GPX8</i>	0.9147
<i>RICTOR</i>	0.8692
<i>DCBLD1</i>	0.9118
<i>KIF6</i>	0.8685
<i>USP49</i>	0.8692
<i>DLC1</i>	0.913
<i>ADCY1</i>	0.8694
<i>TP53INP1</i>	0.8685
<i>KIAA1958</i>	0.9225
<i>STRBP</i>	0.9147
<i>HDX</i>	0.9151
<i>BRWD3</i>	0.8685
<i>SLITRK5</i>	0.9226
<i>CFL2</i>	0.8691
<i>SUGT1</i>	0.9162
<i>PGM2L1</i>	0.9154
<i>SLC16A9</i>	0.9141
<i>AMER2</i>	0.8695
<i>PDZD8</i>	0.8692
<i>FAM204A</i>	0.8696
<i>CLEC1B</i>	0.9142
<i>FUNDC2</i>	0.8689
<i>AGBL2</i>	0.919
<i>CPSF2</i>	0.9162
<i>ARL5B</i>	0.8689
<i>ADAMTS15</i>	0.9135
<i>HIF1AN</i>	0.9226
<i>SPINT1</i>	0.9096
<i>ARIH1</i>	0.9237
<i>SYNPQ2L</i>	0.9135
<i>TRIM44</i>	0.8696
<i>TPP1</i>	0.9134
<i>TRIM66</i>	0.8692
<i>PRTG</i>	0.9225
<i>PKD1L2</i>	0.9138
<i>NA</i>	0.9224
<i>TMED3</i>	0.8696

<i>GALR1</i>	0.9161
<i>TVP23A</i>	0.9143
<i>SLFN5</i>	0.8689
<i>GREM1</i>	0.8696
<i>SGSM1</i>	0.9145
<i>PBX3</i>	0.9124
<i>FBXO22</i>	0.9162
<i>IRGQ</i>	0.916
<i>ZNF226</i>	0.9155
<i>ANKRD11</i>	0.8691
<i>ZNF641</i>	0.9223
<i>TTYH1</i>	0.9213
<i>MAPK1IP1L</i>	0.9159
<i>POLR3D</i>	0.9216
<i>FAM84B</i>	0.9151
<i>TET2</i>	0.9152
<i>ANKRD49</i>	0.914
<i>IRS1</i>	0.8688
<i>MECP2</i>	0.8692
<i>RAB3B</i>	0.8696
<i>SH3TC2</i>	0.8694
<i>SHE</i>	0.8688
<i>PTAFR</i>	0.9212
<i>HIC2</i>	0.923
<i>TOR1AIP2</i>	0.8691
<i>MAP3K2</i>	0.869
<i>TMEM154</i>	0.8695
<i>GPR37L1</i>	0.8689
<i>TMEM192</i>	0.9225
<i>NIPA1</i>	0.9152
<i>RNF150</i>	0.9161
<i>USP38</i>	0.9233
<i>CRTAP</i>	0.8687
<i>KRT78</i>	0.9121
<i>LONRF2</i>	0.8692
<i>SERPINB9</i>	0.9147
<i>NUDCD2</i>	0.9224
<i>SGCD</i>	0.8692

<i>ATF7</i>	0.9155
<i>TMEM126B</i>	0.911
<i>NETO2</i>	0.8688
<i>CLCN5</i>	0.9239
<i>KCND3</i>	0.8687
<i>ZNF562</i>	0.8695
<i>GATM</i>	0.9106
<i>SYNPO</i>	0.9148
<i>ZNF556</i>	0.9156
<i>NEGR1</i>	0.8696
<i>DPAGT1</i>	0.9135
<i>ALG14</i>	0.9161
<i>ARNT2</i>	0.9155
<i>FUT9</i>	0.8695
<i>ZNF24</i>	0.869
<i>PDP2</i>	0.8689
<i>FAM222B</i>	0.9144
<i>BNC2</i>	0.8694
<i>PARP14</i>	0.9151
<i>TNKS</i>	0.8688
<i>STOX2</i>	0.8686
<i>SMARCC1</i>	0.9135
<i>ZNF417</i>	0.9126
<i>PEAK1</i>	0.9162
<i>NABP1</i>	0.916
<i>XCR1</i>	0.9155
<i>RNF213</i>	0.8689
<i>PHC3</i>	0.9161
<i>CBX2</i>	0.9148
<i>SWSAP1</i>	0.9097
<i>CD34</i>	0.8687
<i>CYB561D1</i>	0.8686
<i>MGA</i>	0.9156
<i>ATP2A2</i>	0.9155
<i>CNTNAP2</i>	0.8685
<i>IGDCC3</i>	0.9216
<i>MYO1H</i>	0.9103
<i>SLCO2A1</i>	0.9126

<i>TMEM167A</i>	0.8687
<i>SH3PXD2B</i>	0.8687
<i>C4orf32</i>	0.8692
<i>FZD4</i>	0.8685
<i>PDE12</i>	0.916
<i>CA5A</i>	0.916
<i>VCPIP1</i>	0.8691
<i>YPEL2</i>	0.915
<i>CADM2</i>	0.869
<i>SMAD2</i>	0.9162
<i>EIF3F</i>	0.9155
<i>ALG10B</i>	0.8695
<i>RPS6KB2</i>	0.9185
<i>MLXIP</i>	0.9157
<i>SLC35E3</i>	0.8696
<i>ZDHHC21</i>	0.8694
<i>JAKMIP2</i>	0.8689
<i>SPRYD4</i>	0.9162
<i>RNF152</i>	0.916
<i>ZNF843</i>	0.9137
<i>MTX3</i>	0.9153
<i>SLC38A9</i>	0.9127
<i>POLE</i>	0.8693
<i>SCN4B</i>	0.9146
<i>RIMKLA</i>	0.8691
<i>RPS6KA3</i>	0.9153
<i>HIC1</i>	0.915
<i>PAWR</i>	0.9159
<i>MIEF2</i>	0.9133
<i>SAMD12</i>	0.916
<i>IL17RA</i>	0.8687
<i>ARL6IP6</i>	0.9131
<i>AMER3</i>	0.9146
<i>NT5DC1</i>	0.8689
<i>CSRNP3</i>	0.8693
<i>PXT1</i>	0.9124
<i>CLK3</i>	0.8696
<i>ARID3B</i>	0.9221

<i>C14orf28</i>	0.9215
<i>ZNF154</i>	0.8686
<i>SOCS4</i>	0.9221
<i>FGD6</i>	0.869
<i>PLD5</i>	0.9159
<i>ZNF609</i>	0.869
<i>TSPYL5</i>	0.9146
<i>YOD1</i>	0.9146
<i>GPR157</i>	0.9144
<i>LRRC57</i>	0.916
<i>AEN</i>	0.9132
<i>NME9</i>	0.9126
<i>ZNF678</i>	0.922
<i>RFX7</i>	0.869
<i>RNF41</i>	0.8688
<i>RTKN2</i>	0.8685
<i>MGAT4C</i>	0.8697
<i>CREB3L2</i>	0.9159
<i>RGMA</i>	0.8695
<i>HHIPL1</i>	0.9156
<i>FIGN</i>	0.9237
<i>PLCXD1</i>	0.9155
<i>MXRA7</i>	0.9158
<i>PAPPA</i>	0.9223
<i>C16orf72</i>	0.9224
<i>PLCXD3</i>	0.9156
<i>CEP63</i>	0.9151
<i>GJC1</i>	0.9157
<i>CALN1</i>	0.8694
<i>POTEC</i>	0.9218
<i>ZNF623</i>	0.8688
<i>MACC1</i>	0.8686
<i>KREMEN1</i>	0.9154
<i>KCTD16</i>	0.8695
<i>B3GALT5</i>	0.9162
<i>TMPRSS2</i>	0.9123
<i>FAM120C</i>	0.8688
<i>GOLGA6L4</i>	0.9143

<i>PCDH9</i>	0.9162
<i>SDR42E1</i>	0.9225
<i>FLRT2</i>	0.9162
<i>FAM43A</i>	0.9107
<i>PURA</i>	0.8695
<i>ZBTB37</i>	0.9237
<i>TNFAIP8L1</i>	0.9139
<i>RAD51D</i>	0.8695
<i>IFNLR1</i>	0.9145
<i>BRCC3</i>	0.9122
<i>LSAMP</i>	0.8693
<i>LMLN</i>	0.9158
<i>PBX1</i>	0.9158
<i>C16orf52</i>	0.9146
<i>YTHDF3</i>	0.8686
<i>PIGP</i>	0.8693
<i>IKZF1</i>	0.8687
<i>PTCH1</i>	0.9161
<i>CYP2R1</i>	0.9128
<i>MARC1</i>	0.8688
<i>ZNF555</i>	0.8686
<i>KPNA4</i>	0.9225
<i>FSD2</i>	0.8686
<i>PPARA</i>	0.9161
<i>NAP1L1</i>	0.9226
<i>SESTD1</i>	0.8691
<i>TET3</i>	0.9221
<i>LIN28B</i>	0.9235
<i>TMEM256- PLSCR3</i>	0.9117
<i>FAM122A</i>	0.9151
<i>SHISA7</i>	0.8688
<i>ZC3H6</i>	0.9161
<i>NCR3LG1</i>	0.869
<i>ZNF793</i>	0.8685
<i>ZNF383</i>	0.8689
<i>CENPP</i>	0.8687
<i>RALGAPA2</i>	0.9144

<i>ASAH2</i>	0.9151
<i>PTAR1</i>	0.9224
<i>PARVB</i>	0.8688
<i>VWC2</i>	0.8694
<i>SNTN</i>	0.9217
<i>BEND4</i>	0.916
<i>NA</i>	0.9137
<i>PTPLAD2</i>	0.9225
<i>KCTD21</i>	0.9122
<i>NDUFA4</i>	0.9197
<i>FAM179A</i>	0.9159
<i>PTPRT</i>	0.9158
<i>PLEKHG4</i>	0.8685
<i>RYR1</i>	0.8686
<i>SRGAP3</i>	0.9157
<i>LCOR</i>	0.8691
<i>FUT4</i>	0.8685
<i>ZNF774</i>	0.8692
<i>ZNF765</i>	0.9225
<i>TSC22D2</i>	0.869
<i>ZNF605</i>	0.8693
<i>IPO4</i>	0.9148
<i>GDAP2</i>	0.9224
<i>TPK1</i>	0.9138
<i>MAN2A2</i>	0.9145
<i>HDAC2</i>	0.869
<i>SLC22A25</i>	0.9138
<i>WNK3</i>	0.8687
<i>ZKSCAN5</i>	0.8685
<i>TECPR2</i>	0.9152
<i>ZNF512B</i>	0.9213
<i>ZNF431</i>	0.9225
<i>NF1</i>	0.8687
<i>COL27A1</i>	0.9144
<i>POTEI</i>	0.9142
<i>NHLRC2</i>	0.9162
<i>FLNA</i>	0.8692
<i>SRGAP1</i>	0.9226

<i>LRRC8B</i>	0.8688
<i>NOL4L</i>	0.8686
<i>C6orf141</i>	0.9121
<i>DDI2</i>	0.8689
<i>TRIM33</i>	0.8685
<i>LRP10</i>	0.9151
<i>CDC42SE1</i>	0.9144
<i>EME2</i>	0.915
<i>ZNF81</i>	0.8687
<i>ERO1L</i>	0.9154
<i>PLCG2</i>	0.9154
<i>FCHSD1</i>	0.9198
<i>ZNF121</i>	0.869
<i>MBP</i>	0.8694
<i>MRPL42</i>	0.8696
<i>ZNF248</i>	0.9149
<i>CACNA1E</i>	0.8695
<i>HELZ</i>	0.9161
<i>ZKSCAN8</i>	0.8691
<i>ASPH</i>	0.8691
<i>ZNF26</i>	0.8696
<i>NRARP</i>	0.9106
<i>ZNF587</i>	0.9158
<i>MDM4</i>	0.9162
<i>IPO9</i>	0.9158
<i>SLC5A3</i>	0.8693
<i>CNOT7</i>	0.8691
<i>LRIG2</i>	0.8695
<i>MAP3K3</i>	0.9135
<i>ATG9A</i>	0.9146
<i>EFCAB2</i>	0.8689
<i>CHIC1</i>	0.9155
<i>PHACTR4</i>	0.9148
<i>PBX2</i>	0.9108
<i>FAM155A</i>	0.8692
<i>PSORS1C2</i>	0.9099
<i>FBXO48</i>	0.8689
<i>PCDHA4</i>	0.9224

<i>TRIM13</i>	0.9158
<i>SLC35B4</i>	0.915
<i>ZBTB10</i>	0.9158
<i>TMEM170B</i>	0.8689
<i>GPR56</i>	0.9148
<i>C15orf59</i>	0.9153
<i>C5orf51</i>	0.9156
<i>ONECUT3</i>	0.9158
<i>NYNRIN</i>	0.9194
<i>ATP10A</i>	0.8686
<i>PBX2</i>	0.9108
<i>PSORS1C2</i>	0.9105
<i>VGLL3</i>	0.8695
<i>TRIM71</i>	0.9239
<i>METTL6</i>	0.9151
<i>XKR4</i>	0.9162
<i>PRR22</i>	0.9135
<i>C17orf51</i>	0.869
<i>FGFR10P</i>	0.8696
<i>GIMAP1</i>	0.9148
<i>NRAS</i>	0.915
<i>SYNJ2BP</i>	0.916
<i>LEPROT</i>	0.8687
<i>RPS29</i>	0.8691
<i>ZNF891</i>	0.9226
<i>VSTM5</i>	0.9139
<i>PEX26</i>	0.9237
<i>SIAH3</i>	0.9158
<i>CCDC7</i>	0.9141
<i>PLXNA4</i>	0.916
<i>APOL6</i>	0.8693
<i>PBX2</i>	0.9108
<i>PBX2</i>	0.9108
<i>PSORS1C2</i>	0.9105
<i>PBX2</i>	0.9108
<i>PSORS1C2</i>	0.9105
<i>KIAA0040</i>	0.8685
<i>PBX2</i>	0.9108

<i>ARHGEF38</i>	0.9146	<i>ZNF432</i>	0.9142	<i>TRABD2B</i>	0.8689
<i>TMEM189</i>	0.8693	<i>CUX1</i>	0.8695	<i>SLC25A53</i>	0.8687
<i>ARHGAP8</i>	0.9207	<i>P2RX5-TAX1BP3</i>	0.8686	<i>NUDT3</i>	0.8694
<i>AMACR</i>	0.913	<i>ITGB3</i>	0.9139	<i>GRIN2B</i>	0.9226
<i>PEG10</i>	0.9158	<i>NA</i>	0.9149	<i>ZBTB8B</i>	0.9225
<i>NA</i>	0.9113	<i>RBM15B</i>	0.8685	<i>SOCS7</i>	0.8689
<i>MARS2</i>	0.9106	<i>XKR7</i>	0.8688	<i>GOLGA6L9</i>	0.9147
<i>PRR5-ARHGAP8</i>	0.9092	<i>TMEM178B</i>	0.9225	<i>ZNF280B</i>	0.9147
<i>FMN1</i>	0.8694	<i>GAN</i>	0.924	<i>DDTL</i>	0.9107
<i>DNAH10OS</i>	0.8686	<i>NA</i>	0.8687	<i>TTYH1</i>	0.9135
<i>PCDHA10</i>	0.8693	<i>NA</i>	0.9139	<i>TTYH1</i>	0.9135
<i>ATXN7L3B</i>	0.9224	<i>C19orf84</i>	0.9112	<i>NA</i>	0.9141
<i>NA</i>	0.8685	<i>RNF115</i>	0.8695	<i>RBFOX2</i>	0.8688
<i>SOGA3 KIAA0408</i>	0.9224	<i>ZNF850</i>	0.9156	<i>ZNF8</i>	0.9161
<i>NOX5</i>	0.8689	<i>NA</i>	0.9201		

Table I: miRNAs implicated in the pathogenesis of glioblastoma.

hsa-let-7a-1	hsa-mir-137	hsa-mir-181b-2	hsa-mir-21	hsa-mir-30c-1	
hsa-let-7a-2	hsa-mir-139	hsa-mir-181c	hsa-mir-210	hsa-mir-30c-2	hsa-mir-455
hsa-let-7a-3	hsa-mir-142	hsa-mir-181d	hsa-mir-218-1	hsa-mir-31	hsa-mir-486
hsa-let-7d	hsa-mir-143	hsa-mir-183	hsa-mir-218-2	hsa-mir-3163	hsa-mir-491
hsa-mir-101-1	hsa-mir-145	hsa-mir-184	hsa-mir-22	hsa-mir-32	hsa-mir-504
hsa-mir-101-2	hsa-mir-146a	hsa-mir-18a	hsa-mir-221	hsa-mir-323a	hsa-mir-539
hsa-mir-106a	hsa-mir-146b	hsa-mir-193a	hsa-mir-222	hsa-mir-323b	hsa-mir-7-1
hsa-mir-10a	hsa-mir-148a	hsa-mir-195	hsa-mir-224	hsa-mir-326	hsa-mir-7-2
hsa-mir-10b	hsa-mir-149	hsa-mir-196b	hsa-mir-23b	hsa-mir-328	hsa-mir-7-3
hsa-mir-124-1	hsa-mir-151a	hsa-mir-19a	hsa-mir-25	hsa-mir-329-1	hsa-mir-708
hsa-mir-124-2	hsa-mir-153-1	hsa-mir-19b-1	hsa-mir-26a-1	hsa-mir-329-2	hsa-mir-873
hsa-mir-124-3	hsa-mir-153-2	hsa-mir-19b-2	hsa-mir-26a-2	hsa-mir-342	hsa-mir-885
hsa-mir-125b-1	hsa-mir-155	hsa-mir-200	hsa-mir-27b	hsa-mir-34a	hsa-mir-9-1
hsa-mir-125b-2	hsa-mir-15a	hsa-mir-200b	hsa-mir-29a	hsa-mir-367	hsa-mir-9-2
hsa-mir-1260a	hsa-mir-16-1	hsa-mir-205	hsa-mir-29c	hsa-mir-376a-1	hsa-mir-9-3
hsa-mir-128-1	hsa-mir-16-2	hsa-mir-206	hsa-mir-302a	hsa-mir-376a-2	hsa-mir-92a-1
hsa-mir-128-2	hsa-mir-17	hsa-mir-208a	hsa-mir-302b	hsa-mir-381	hsa-mir-92a-2
hsa-mir-1305	hsa-mir-181a-1	hsa-mir-208b	hsa-mir-302c	hsa-mir-425	hsa-mir-95
hsa-mir-130a	hsa-mir-181a-2	hsa-mir-20a	hsa-mir-302d	hsa-mir-451a	hsa-mir-99a
hsa-mir-134	hsa-mir-181b-1	hsa-mir-20b	hsa-mir-30a	hsa-mir-452	

The genes with remarkable expression profile differences between glioblastoma and normal brain tissues among glioblastoma-associated ceRNAs involving T-UCR were defined. Expression of PBX3 gene was significantly higher and NRXN3 gene expression was remarkably lower in glioblastoma than in normal brain tissues according to the current analysis. On the other hand, the other genes did not show any remarkable expression differences (Table III).

Table II: The glioblastoma-associated ceRNAs that match the genes containing T-UCR in the exonic regions.

uc.378	251	<i>NRXN3</i>
uc.184	230	<i>CPEB4</i>
uc.33	312	<i>PTBP2</i>
uc.414	246	<i>THRA</i>
uc.280	220	<i>PBX3</i>
uc.393	275	<i>CLK3</i>

Table III: Expression values of ceRNAs with T-UCR that are associated with glioblastoma in normal brain tissues and glioblastoma.

<i>NRXN3</i> *	1.84	18.41
<i>CPEB4</i>	14.04	11.54
<i>PTBP2</i>	12.1	11.96
<i>THRA</i>	99.62	144.88
<i>PBX3</i> *	19.54	3.29
<i>CLK3</i>	32.92	29.86

*Shows remarkably differential expression profile between normal brain tissues and glioblastoma

The statistical analysis of the relationship between PBX3 and NRXN3 genes and glioblastoma multiforme was carried out via GEPIA database. It was determined that PBX3 and NRXN3 genes were significantly correlated with glioblastoma based on the Spearman correlation analysis (Figure 1) ($p=0.0014$; $R=-0.17$).

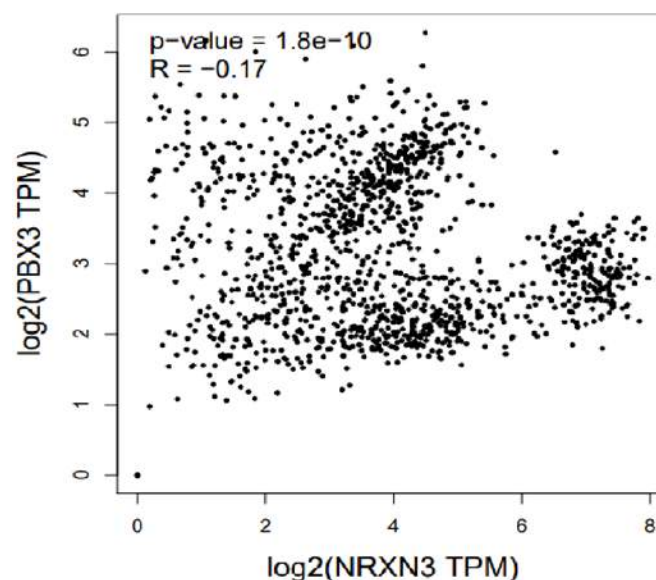


Figure 1: The relationship of NRXN3 and PBX3 genes with glioblastoma.

DISCUSSION

Glioblastoma which is the most frequent and aggressive form of primary malignancies in adult human brains is characterized by tumor heterogeneity, diffuse invasion, drug resistance, and rapid growth. It has been clarified that miRNAs are implicated in tumorigenesis. Moreover, it has been observed that expression levels of miRNAs are differed between pathological and normal tissues. Recent studies have subclassified glioblastoma into five clinically and genetically distinct subtypes according to miRNA expression profiles and it has been supposed that miRNAs are important for the phenotypic characteristics of the subclasses^{16,17}. The median survival time of patients with GBM is approximately 14 to 16 months despite standard treatment options and there is no cure at present. In recent years,

studies in this field have been focused on the identification of new targets for diagnostics and therapeutics for GBM. It is supposed that detection and quantifying miRNAs in serum and tissues will become a standard tool for diagnosis and prognosis of GBM and have a great potential for personalized treatment strategies¹⁸. In this regard, based on the idea that miRNAs are implicated in the pathogenesis of glioblastoma, we aimed to determine novel molecular biomarkers for GBM through *in silico* analysis that uses glioblastoma-specific microRNAs, identifies their combinatorial target genes which have potential ceRNA activities. In this study, 118 microRNAs correlated with glioblastoma were obtained from miRTarBase database (Table I). The genes with ComiR score greater than 0.8685 were listed through 1016 genes that are simultaneously targeted by these 118 miRNAs. The genes with T-UCR in their exonic regions were selected based on the study of Bejerano et al.¹⁴. Subsequently, the genes which show potential ceRNA activities were extracted (Table II). Then, the genes with remarkable expression differences between GBM and normal brain tissues were extracted from glioblastoma-associated ceRNAs that include T-UCR. While PBX3 gene was highly expressed in GBM than in normal brain tissues, NRXN3 gene was significantly less expressed in GBM than in normal brain tissues according to the analysis in this study. On the other hand, other genes did not show any significant differences in expression pattern. According to the findings of the Spearman correlation analysis, PBX3 and NRXN3 genes were shown to have remarkable relationship with GBM.

PBX3 is a member of Pre-B-cell leukemia homeobox family and implicated in early development and several biological processes in adulthood. The location of PBX3 gene is on chromosome 9q33.3. PBX3 as a transcription factor shows a stable interaction with DNA and

binds to DNA with a consensus sequence (TGATTGATTTGAT). It has been demonstrated that PBX3 is commonly associated with cancer and overexpressed in several types of cancers such as hematological malignancies and colorectal cancers. Moreover, PBX3 activates numerous signaling pathways such as MAPK/ERK signaling pathway. PBX3 functions as an oncogene and is implicated in the regulation of biological functions such as stimulating proliferation, colony formation, cell survival, and invasion^{19,20}. It has been demonstrated that PBX3 is upregulated in gastric cancer cells and apoptosis is induced by targeting PBX3 gene in gastric cancer²⁰. In a study conducted with glioma cell lines, it has been shown that PBX3 was overexpressed²¹. Xu et al. reported that PBX3 was significantly associated with invasion of GBM cells and mesenchymal transition²².

Neurexins (NRXNs) are a family of neuronal-specific cell surface proteins and they are implicated in cell recognition and adhesion. Moreover, the presynaptic terminal proteins are involved in synaptogenesis, neurotransmitter release and synaptic transmission and are also essential for the development and function of synapses. NRXN genes are differentially spliced into numerous isoforms^{23,24}. It is known that FoxQ1 as a potential oncogene may induce tumor cell proliferation and migration by targeting NRXN3 gene in a direct way²⁵. It has been reported that FoxQ1 stimulated cell proliferation and migration of glioma by suppressing NRXN3 gene and suggested that NRXN3 gene might be a tumor suppressor²⁴. In the study conducted with breast cancer patients, G allele carriers in rs10146997 of NRXN3 gene was statistically related to the development of breast cancer²⁶. It has been reported that NRXN3 gene expression was downregulated in the samples of GBM²⁷.

NRXN3 and PBX3 genes were associated with GBM in this present study and they were

suggested to have potential roles in carcinogenesis. It has been supposed that NRXN3 acts as a tumor suppressor gene and its expression is decreased in GBM according to the analysis in this study. On the other hand, PBX3 gene is suggested to function as an oncogene and is upregulated in GBM according to the *in silico* analysis.

CONCLUSION

The present study investigated the correlation of NRXN3 and PBX3 genes with GBM and this study supports the potential roles for the genes in the pathogenesis of glioblastoma. Additionally, further *in vivo* and *in vitro* studies are needed in order to elucidate tumor suppressor role of NRXN3 and oncogenic activity of PBX3 in GBM.

Ethics Committee Approval: This study did not require any ethical approval.

Declaration of Conflicting Interests: The authors declare that they have no conflict of interest.

Financial Disclosure: No financial support was received.

REFERENCES

1. Yool AJ, Ramesh S. Molecular targets for combined therapeutic strategies to limit glioblastoma cell migration and invasion. *Front Pharmacol.* 2020; 11: 358.
2. Haar CP, Hebbar P, Wallace GC, et al. Drug resistance in glioblastoma: A mini review. *Neurochem Res.* 2012; 37: 1192-200.
3. Yilmaz A, Altug F, Duz E, et al. Treatment options and effects of survival in glioblastoma multiforme. *J Kartal TR.* 2012; 23: 25-9.
4. Laffont B, Rayner KJ. MicroRNAs in the pathobiology of atherosclerosis. *CJC.* 2017; 33: 313-24.
5. invasion program in glioblastoma. *J Exp Clin Cancer Res.* 2019; 38.
5. Witwer KW, Halushka MK. Toward the promise of microRNAs- Enhancing reproducibility and rigor in microRNA research. *RNA Biol.* 2016; 13: 1103-16.
6. Sherin K, Nair AS. Review of computational prediction of competing endogenous RNA. *J Proteom Bioinform.* 2019; 12.
7. Qi M, Yu B, Yu H, et al. Integrated analysis of a ceRNA network reveals potential prognostic lncRNAs in gastric cancer. *Cancer Med.* 2020; 9: 1798-817.
8. Fassan M, Dall'Olmo L, Galasso M, et al. Transcribed ultraconserved noncoding RNAs (T-UCRs) are involved in Barrett's esophagus carcinogenesis. *Oncotarget.* 2014; 5: 7162-71.
9. Huang HY, Lin YCD, Li J, et al. miRTarBase 2020: updates to the experimentally validated microRNA-target interaction database. *Nucleic Acids Res.* 2020; 48: D148-D154.
10. Ergun S. *In silico* analysis of biomarker potentials of miRNA-mediated ceRNAs in prostate cancer. *Dicle Med J.* 2018; 45: 415-29.
11. Coronello C, Benos PV. ComiR: combinatorial microRNA target prediction tool. *Nucleic Acids Res.* 2013; 41: W159-W164.
12. Us Altay D, Ergun S. *In silico* analysis of biomarker potentials of miRNA mediated ceRNAs in gastric neoplasms. *MBSJHS.* 2019; 5: 106-19.
13. Avsar O. Analysis of miRNA-mediated ceRNAs in the pathogenesis of renal cell carcinoma: An *in silico* approach. *HJSE.* 2020; 7: 223-38.
14. Bejerano G, Pheasant M, Makunin I, et al. Ultraconserved elements in the human genome. *Science.* 2004; 304:1321-5.
15. Tang Z, Li C, Kang B, et al. GEPIA: a web server for cancer and normal gene expression profiling and interactive analysis. *Nucleic Acids Res.* 2017; 45: W98-W102.
16. Zhao Y, Huang W, Kim TM, et al. MicroRNA-29a activates a multi-component growth and
17. Touat M, Idbaih A, Sanson M, et al. Glioblastoma targeted therapy: updated approaches from recent biological insights. *Ann Oncol.* 2017; 28: 1457-72.

18. Shea A, Harish V, Afzal Z, et al. MicroRNAs in glioblastoma multiforme pathogenesis and therapeutics. *Cancer Med.* 2016; 5: 1917-46.
19. Morgan R, Pandha HS. PBX3 in cancer. *Cancers.* 2020; 12.
20. Li YS, Zou Y, Dai DQ. MicroRNA-320a suppresses tumor progression by targeting PBX3 in gastric cancer and is downregulated by DNA methylation. *World J Gastrointest Oncol.* 2019; 11: 842-56.
21. Pan C, Gao H, Zheng N, et al. Mir-320 inhibits the growth of glioma cells through downregulating PBX3. *Biol Res.* 2017; 50.
22. Xu X, Bao Z, Liu Y, et al. PBX3/MEK/ERK1/2/LIN28/let-7b positive feedback loop enhances mesenchymal phenotype to promote glioblastoma migration and invasion. *J Exp Clin Cancer Res.* 2018; 37: 158.
23. Harkin LF, Lindsay SJ, Xu Y, et al. Neurexins 1-3 each have a distinct pattern of expression in the early developing human cerebral cortex. *Cereb Cortex.* 2017; 27: 216-32.
24. Sun HT, Cheng SX, Tu Y, et al. FoxQ1 promotes glioma cells proliferation and migration by regulating NRXN3 expression. *PLoS One.* 2013; 8: e55693.
25. Xiang XJ, Deng J, Liu YW, et al. Mir-1271 inhibits cell proliferation, invasion and EMT in gastric cancer by targeting FOXQ1. *Cell Physiol Biochem.* 2015; 36: 1382-94.
26. Kusinska R, Gorniak P, Pastorczak A, et al. Influence of genomic variation in FTO at 16q12.2, MC4R at 18q22 and NRXN3 at 14q31 genes on breast cancer risk. *Mol Biol Rep.* 2012; 39: 2915-19.
27. Yang Q, Wang R, Wei B, et al. Gene and microRNA signatures are associated with the development and survival of glioblastoma patients. *DNA Cell Biol.* 2019; 38: 688-99.